

## Cascading Fermi Resonances and the Soft Mode in Dense Ice

Viktor V. Struzhkin,\* Alexander F. Goncharov, Russell J. Hemley, and Ho-kwang Mao  
*Geophysical Laboratory and Center for High Pressure Research, Carnegie Institution of Washington,  
 5251 Broad Branch Road, N.W., Washington, D.C. 20015*  
 (Received 11 March 1997)

Synchrotron infrared reflectance and absorbance spectroscopy reveals a cascading sequence of pressure-induced Fermi resonances in compressed H<sub>2</sub>O and D<sub>2</sub>O ices up to and through the transition to the symmetric hydrogen-bonded phase. These resonances arise from the extremely large pressure shift of the O-H(D) stretching mode associated with the transition, which causes multiple avoided crossings between this and other infrared-active vibrational states. The highest frequency LO mode has a minimum at the transition, and the LO-TO splitting increases dramatically in the high-pressure phase. Fano-like features are present in absorbance even in the absence of mode coupling. [S0031-9007(97)03301-2]

PACS numbers: 63.20.Dj, 62.50.+p, 77.80.Bh

The vibrational dynamics of compressed H<sub>2</sub>O ice is a casebook example of a many-body quantum system in condensed matter. Recent high-pressure experiments have revealed a wealth of new phenomena about the dynamics of this system at megabar pressures. Infrared reflectivity measurements demonstrate that the softening of the O-H(D) stretching modes, previously documented at lower pressures (e.g., Refs. [1–3]), is profound in this pressure range. The frequencies of the infrared modes decrease from 3150–3220 cm<sup>-1</sup> (ice I at zero pressure) to ~1500 cm<sup>-1</sup> at 60 GPa (in ice VII), followed by a hardening of the stretching mode at higher pressure [4]. This result provided direct evidence for the transition [4] to the nonmolecular phase with symmetric hydrogen bonds [5]. Although confirmed by conventional infrared absorption measurements [6] and in good agreement with theoretical predictions [7], numerous vibrational properties of ice in the vicinity of the transition are not understood. Prior to the transition, the soft stretching mode exhibits a pressure-induced Fermi resonance, but the results for H<sub>2</sub>O [4] and HDO [8] differ, and both the complexity of the spectra and absorption by the diamond anvils complicated detailed study of this effect. Evidence for a Fano resonance between a rotational mode and the broad continuum originating from the soft mode has also been reported [9], but its origin and relationship to the phase transition need to be examined. Further, the system is expected to be strongly anharmonic near the transition, exhibiting both dynamical disorder and quantum effects (tunneling) associated with the proton motion [4,7,10].

We present synchrotron infrared absorption and reflectivity spectra of protonated and deuterated ices that unexpectedly reveal a cascading series of Fermi resonances between the soft stretching mode and other excitations. This phenomenon arises from the strong pressure dependence of the soft mode, which interacts sequentially with other excitations having weak pressure dependencies. We introduce a simple model for these multiple resonances and obtain the pressure dependence of the bare soft mode,

which provides a more accurate estimate of the transition pressure. The highest frequency LO mode has a minimum at the transition, and there is a large LO-TO splitting (1600 cm<sup>-1</sup>) of the stretching mode at the highest pressures. Fano-like line shape features in high-pressure absorbance spectra result from complex behavior of the optical response even in the absence of coupling between modes.

There are two main difficulties in high-pressure studies of O-H(D) excitations in the diamond cell. First, the O-H stretching modes are so intense that the absorbance maxima typically saturate for sample thicknesses appropriate for measurement of bulk absorption properties. Second, the transmission through the diamond anvils (typically 2.5 mm thickness) is 0.05% in the region of second-order diamond absorption (1900–2100 cm<sup>-1</sup>), precluding measurements in a crucial spectral region. These difficulties were resolved in this study by measuring both reflectivity and absorption of H<sub>2</sub>O and D<sub>2</sub>O ices with an intense synchrotron infrared source, combined with the use of thin (1.2 mm thick) anvils allowing 3% transmission in the diamond second-order absorption region. Reflectivity measurements (ideal for strong features) and absorption (for the weaker features) were thus measured over the entire range from 600 to 10 000 cm<sup>-1</sup> [11]. Representative spectra of H<sub>2</sub>O are shown in Fig. 1. The spectra were fit using a classical oscillator model [12] (see also, Ref. [4]). The peak positions as a function of pressure obtained from analyses are shown in Fig. 2. There is no evidence for structural phase transitions to 60 GPa [4,13]. Rather, we can understand the emergent complexity in the spectra by considering the symmetries and interactions between vibrational states.

The high-frequency O-H stretching vibrations in H<sub>2</sub>O ice VII form a triplet (a doublet and a small shoulder) up to 25 GPa and exhibit soft-mode behavior with increasing pressure. Using selection rules for ice VIII (point group *D*<sub>4h</sub>) [2,14,15] as in previous work on ice VII [16,17], we can assign the observed doublet to  $\nu_3(E_u)$  and  $\nu_1(A_{2u})$

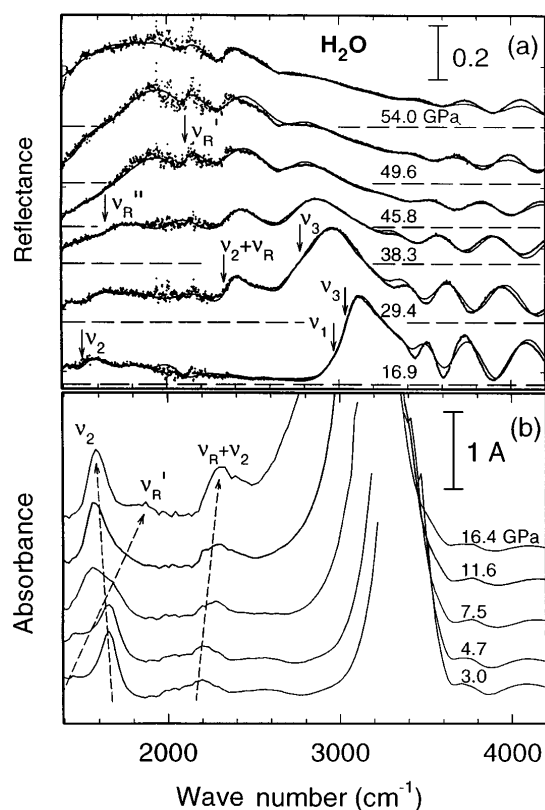


FIG. 1. Synchrotron infrared spectra of H<sub>2</sub>O at 3–55 GPa and 300 K. (a) Reflectivity spectra. Solid lines are oscillator fits (see text); dashed lines are zero lines for the corresponding reflectivity spectra. (b) Absorbance spectra. The oscillations at high frequency are interference fringes created by the diamond cell. Dashed lines with arrows are guides to the eye.

(e.g., measured at 3 GPa by reflectivity at 3350 and 3290 cm<sup>-1</sup>, respectively). We observe four absorption bands at intermediate frequencies, {e.g., 1000–2200 cm<sup>-1</sup> at 3.0 GPa [Fig. 1(b)]}. The 1600 cm<sup>-1</sup> band is the bending mode  $\nu_2(A_{2u})$ . To assign the other bands, we note that the lowest frequency modes are the well-established rotational  $\nu_{R_x,R_y}(E_u)$  and translational  $\nu_{T_x,T_y}(E_u)$  vibrations [15,18]. We use the symmetries and selection rules for overtones and combinations of these modes [19] at the  $\Gamma$  point of the Brillouin zone for ice VIII [20]. A general result of this analysis is that overtones of the ir-active modes have “gerade” symmetry and thus are ir inactive, consistent with our measurements. As such, the band labeled  $\nu_2 + \nu_R$  (2200 cm<sup>-1</sup> in H<sub>2</sub>O at 3.5 GPa; 1600 cm<sup>-1</sup> in D<sub>2</sub>O at 3 GPa) arises from the  $\nu_2(A_{1g}) + \nu_{R_x,R_y}(E_u)$  combination. The bands designated  $\nu_R'$  and  $\nu_R''$  (1000 and 1450 cm<sup>-1</sup> in H<sub>2</sub>O at 3.5 GPa; 760 and 1030 cm<sup>-1</sup> in D<sub>2</sub>O at 3 GPa) are combinations of the lowest and highest ir-active  $\nu_{R_x,R_y}(E_u)$  modes, respectively, with the lowest and highest Raman-active  $\nu_{R_x,R_y}(E_g)$  modes [15].

The pressure-induced changes in frequencies and intensities clearly show evidence for interactions between the vibrations. To examine this, we write the equations of mo-

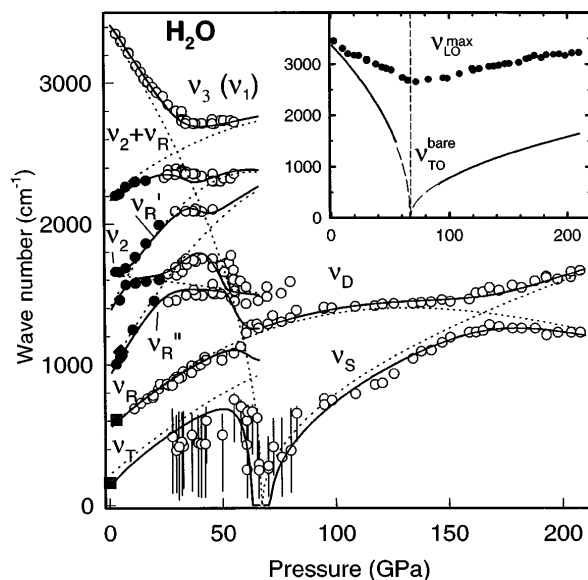


FIG. 2. Vibrational frequencies for H<sub>2</sub>O up to 210 GPa. Closed circles, absorption spectra; open circles, reflectivity spectra. Solid lines are fits to the multiple Fermi resonance model, and the dotted lines are the bare frequencies. Diamond, Ref. [26]; squares, Refs. [15,18]. Inset: Closed circles show the variation of the highest LO frequency with pressure; solid and dashed lines correspond to the bare TO frequency.

tion (Fourier components) for coupled modes [21],

$$(-\omega^2 + i\omega\Gamma_k + \Omega_k^2)x_k + \sum_{n \neq k}^N (i\omega\Gamma_{nk} + \Delta_{nk}^2)x_n = e_k E_\omega. \quad (1)$$

Here the index  $k$  extends from 1 to  $N$ , where  $N$  is the number of vibrations,  $\Omega_k$  are the bare frequencies,  $\Gamma_{nk}$  and  $\Delta_{nk}^2$  are the coupling terms (in general frequency dependent),  $x_k$  are the displacements,  $e_k$  are the reduced effective charges, and  $E_\omega$  is the Fourier component of the external electric field. Neglecting damping (equivalent to the harmonic approximation), we can write a secular equation for the oscillator frequencies modified by interactions  $\Delta_{nk}$ ,

$$|(-\omega^2 + \Omega_k^2)\delta_{nk} + \Delta_{nk}^2| = 0. \quad (2)$$

We solve the determinant in Eq. (2), and fit the observed frequencies by adjusting the nondiagonal matrix elements and parameters for the bare frequencies. For the bare frequency of the soft mode, we use  $\nu = [a(P_c - P)]^{1/2}$ , where  $P_c$  is the transition pressure and  $a$  is a parameter. The bare frequencies of all other modes are taken as second-order polynomials with respect to pressure, with the exception of a third-order polynomial for the rotational mode up to 210 GPa [22]. The resulting fit, including the bare modes, is shown in Fig. 2.

As the transition is approached, the soft mode becomes strongly damped (e.g., Fig. 1). We have examined the effects of possible interactions between the mode and  $\nu_{R_x,R_y}(E_u)$  and  $\nu_{T_x,T_y}(E_u)$  in the model (Fig. 2). In this

region, however, the soft mode cannot be described as an oscillator with constant damping; i.e., the potential for the soft mode is strongly anharmonic, a result that modifies appreciably the dielectric response [23,24]. In support of this, we observe a broad feature near the transition (points above  $\nu_D$  in Fig. 2), which likely arises from excitations to higher energy levels of an anharmonic (e.g., double-well) potential [4]. The soft mode is not observed directly below  $1500 \text{ cm}^{-1}$ , as its intensity begins to be transferred to the low-frequency region below  $600 \text{ cm}^{-1}$  at about 50 GPa (i.e., below the actual phase transition). We suggest that both anharmonicity and strong interaction with the translational mode  $\nu_{Tx,Ty}(E_u)$  are responsible for this effect. Above the transition the system again becomes more harmonic, and our secular determinant has the very simple form,

$$\begin{vmatrix} \omega_S^2 - \omega^2 & \Delta_{SD}^2 \\ \Delta_{SD}^2 & \omega_D^2 - \omega^2 \end{vmatrix}, \quad (3)$$

where the indices  $S$  and  $D$  refer to the stretching and deformational modes, respectively. This expression is similar (but not equivalent) to the empirical perturbation theory analysis of the frequencies of interacting modes in the classical Fermi resonance scheme used for HDO [8]. In contrast to the single resonance reported for HDO [8], our measurements reveal a sequence of mode couplings. Altogether, we find evidence for up to eight resonances (i.e., with  $\Delta_{nk} \neq 0$ ) over the complete range of pressures (Fig. 2).

The behavior of the bare stretching mode gives additional information on the transition. The fit to  $\nu = [a(P_c - P)]^{1/2}$  above and below the transition gives  $a = 1.60 \times 10^5$  and  $a = 1.85 \times 10^4$ , respectively. We find  $P_c = 67(3)$  GPa for the complete softening of the mode in  $\text{H}_2\text{O}$  [ $P_c = 75(3)$  GPa for  $\text{D}_2\text{O}$ ]. Note that the transition-driven soft mode in antiferroelectric phases (like ice VIII) should not be ir active, and normal coordinate analysis [14] indicates that the true symmetry-breaking mode is the Raman-active  $\nu_1(A_{1g})$  vibration. The frequencies of  $\nu_3(E_u)$  and  $\nu_1(A_{2u})$  are quite close, and we expect that  $\nu_1(A_{1g})$  is close to  $\nu_1(A_{2u})$ , but this (as well as modes at  $k \neq 0$ ) should be examined near the transition. We also determined the position of the highest frequency longitudinal mode from the maximum in  $\text{Im}[1/\epsilon(\omega)]$ , where  $\epsilon(\omega)$  was taken from the oscillator fits and Kramers-Kronig analyses of the reflectivity spectra [25]. The transverse (TO) and longitudinal (LO) frequencies,  $\omega_T$  and  $\omega_L$ , are related by

$$\sum_i \omega_{L_i}^2 = \sum_i \omega_{P_i}^2 / \epsilon_\infty + \sum_i \omega_{T_i}^2, \quad (4)$$

where  $\omega_P$  is the plasma frequency. The LO mode has a minimum at the transition point (Fig. 2), which is naturally explained by the minimum in TO frequency. We find a large LO-TO splitting of  $1600 \text{ cm}^{-1}$  at the highest pressure (210 GPa), where the stretching mode

dominates the ir spectrum. In contrast, the LO-TO splitting is  $\sim 100 \text{ cm}^{-1}$  in ice VII below 10 GPa.

Finally, we compare the absorbance spectra determined using our reflectivity data with previous thin film absorption measurements and reported evidence for a Fano resonance based on an asymmetric line shape [9]. We calculated absorbance spectra from our data assuming both independent and coupled oscillators for the stretching and rotational modes with the above model for the interactions [Eq. (1)] [21]. The resulting spectra are in very good agreement with those reported in Ref. [9] (Fig. 3). However, we observe an asymmetric line shape for the rotational mode in absorbance both with and without coupling. This arises from the nonlinear dependence of the refractive index in the vicinity of the rotational mode: even with a Lorentzian line shape for  $\epsilon_2(\omega)$ , the absorption coefficient  $\alpha = \epsilon_2(\omega)\omega/n(\omega)$  is asymmetric due to the fact that the refractive index  $n(\omega)$  has a maximum below the TO frequency of the rotational mode and decreases above it. For example, the maximum and minimum values of  $n(\omega)$  can differ by 300% at 108 GPa. The broad peak just above the rotational mode (attributed to higher-level transitions in anharmonic potential) also contributes to the asymmetry. Thus, we find that a Fano-like profile can be produced even in the absence of a resonance between oscillators.

In conclusion, we observe a striking number of Fermi resonances between the soft antisymmetric stretching mode and the rotational mode, the bending mode, and their combinations, as the soft mode approaches the symmetrization transition. The behavior can be understood in terms of a monotonic decrease of the O-H...O potential barrier that results in the formation of symmetric hydrogen bonds. The same change in the potential

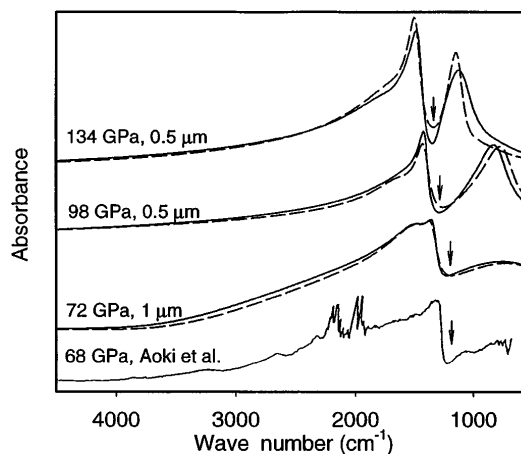


FIG. 3. Representative absorbance spectra determined from the reflectivity spectra. Solid line, coupled oscillators; dashed line, uncoupled oscillators. The bottom curve is from Ref. [9]. The arrow indicates the observed antiresonance. The coupling parameters  $\Delta_{SD}$  [Eq. (3)] for the coupled-oscillator fits are  $450 \text{ cm}^{-1}$  (72 GPa),  $580 \text{ cm}^{-1}$  (98 GPa),  $600 \text{ cm}^{-1}$  (134 GPa). The maximum in absorbance at 134 GPa is 2.5 A.

is responsible for the highly anharmonic response of the stretching mode close to the transition. The large degree of pressure-induced vibrational mode coupling in this system and complex optical response requires considerable care in interpreting its vibrational spectra. The minimum in the highest frequency LO mode at the phase transition arises from the vanishing of the TO mode frequency at the transition. The large LO-TO splitting indicates high ionicity of the high-pressure phase.

We thank R.E. Cohen and M. Somayazulu for discussions. This work was supported by the NSF (DMR-9624050), NASA (NAGW-1722), and the DOE (DE-AC02-76-CH00016; DE-FG02-96ER14651). The Center for High Pressure Research is an NSF Science and Technology Center.

---

\*Permanent address: Inst. for High Pressure Phys., Russ. Acad. of Sci., 142092 Troitsk, Moscow Region, Russia.

- [1] D.D. Klug and E. Whalley, *J. Chem. Phys.* **81**, 1220 (1984).
- [2] K. R. Hirsch and W. B. Holzapfel, *J. Chem. Phys.* **84**, 2771 (1986).
- [3] P. Pruzan, *J. Mol. Struct.* **322**, 279 (1994).
- [4] A. F. Goncharov, V. V. Struzhkin, M. S. Somayazulu, R. J. Hemley, and H. K. Mao, *Science* **272**, 149 (1996).
- [5] W. B. Holzapfel, *J. Chem. Phys.* **56**, 712 (1972).
- [6] K. Aoki, H. Yamawaki, M. Sakashita, and H. Fukithisa, *Phys. Rev. B* **54**, 15 673 (1996).
- [7] C. Lee, D. Vanderbilt, K. Laasonen, R. Car, and M. Parrinello, *Phys. Rev. Lett.* **69**, 462 (1992); *Phys. Rev. B* **47**, 4863 (1993).
- [8] K. Aoki, H. Yamawaki, and M. Sakashita, *Science* **268**, 1322 (1995).
- [9] K. Aoki, H. Yamawaki, M. Sakashita, and H. Fukithisa, *Phys. Rev. Lett.* **76**, 784 (1996).
- [10] F. H. Stillinger and K. S. Schweitzer, *J. Phys. Chem.* **87**, 4281 (1983); K. S. Schweitzer and F. H. Stillinger, *J. Chem. Phys.* **80**, 1230 (1984).
- [11] The measurements were performed on the U2B IR beam line at the National Synchrotron Light Source using a FT-IR (Nicolet 750) spectrometer with KBr beam splitters [4].
- [12] A. S. Barker, Jr., *Phys. Rev.* **136**, A1290 (1964).
- [13] R. J. Hemley *et al.*, *Nature (London)* **330**, 737 (1987); M. Somayazulu *et al.* (to be published). Changes in order-disorder, however, cannot be ruled out.
- [14] P. T. T. Wong and E. Whalley, *J. Chem. Phys.* **64**, 2359 (1976).
- [15] S. P. Tay, D. D. Klug, and E. Whalley, *J. Chem. Phys.* **83**, 2708 (1985).
- [16] M. Gauthier, J. C. Chevrin, and P. Pruzan, *High Press. Res.* **10**, 641 (1992).
- [17] E. Whalley, *Can. J. Chem.* **55**, 3429 (1977).
- [18] M. Kobayashi, *Solid State Phys. (Japan)* **31**, 127 (1996).
- [19] G. F. Koster, J. O. Dimmock, R. G. Wheeler, and H. Statz, *Properties of the Thirty-Two Point Groups* (M.I.T., Cambridge, 1963).
- [20] The model is able to describe the anomalous frequency shifts of all observed excitations, and it was not necessary to take into account multiple excitations with wave vectors  $+\mathbf{k}$ ,  $-\mathbf{k}$  (i.e., away from zone center). Interactions with non-zone-center combination excitations appear to contribute mainly to the linewidths of the observed bands.
- [21] A. S. Barker, Jr. and J. J. Hopfield, *Phys. Rev.* **135**, A1732 (1964).
- [22] We used the following parameters (all frequencies in  $\text{cm}^{-1}$ , pressure in GPa); the number in parentheses is the coupling  $\Delta_{nk}$  [Eq. (2)] to the stretching mode:  $\nu'_R = 960 + 29P - 0.145P^2$  ( $720 \text{ cm}^{-1}$ ),  $\nu''_R = 1390 + 31P - 0.245P^2$  ( $820 \text{ cm}^{-1}$ ),  $\nu_2 = 1640 - 2.0P$  ( $450 \text{ cm}^{-1}$ ),  $\nu_R = 558 + 14.7P - 0.077P^2 + 0.00011P^3$  ( $580 \text{ cm}^{-1}$ ),  $\nu_T = 220 + 14P - 0.05P^2$  ( $750 \text{ cm}^{-1}$ ),  $\nu_2 + \nu_R$  was taken as a sum of  $\nu_2$  and  $\nu_R$  with coupling parameter  $1050 \text{ cm}^{-1}$ ; coupling parameters between the  $\nu_2$  and  $\nu'_R$ ,  $\nu''_R$  are 480 and  $540 \text{ cm}^{-1}$ , respectively.  $\Delta_{nk} = 0$  for all other pairs of modes.
- [23] V. G. Vaks, V. M. Galitskii, and A. I. Larkin, *Sov. Phys. JETP* **24**, 1071 (1967).
- [24] J. W. Flocken, R. A. Guenther, J. R. Hardy, and L. L. Boyer, *Phys. Rev. B* **40**, 11 496 (1989).
- [25] V. V. Struzhkin, A. F. Goncharov, R. J. Hemley, and H. K. Mao (to be published).
- [26] W. B. Holzapfel, D. Seiler, and M. F. Nicol, *Lunar Planet. Sci.* **14**, 321 (1979).